

Halide Ion Addition to Bismuth-Containing Iron Carbonyl Compounds: Synthesis and Characterization of the Two Bridged-Butterfly Cluster Compounds $[\text{Et}_4\text{N}][(\mu\text{-H})\text{Fe}_2(\text{CO})_6\text{Bi}_2\{\mu\text{-Fe}(\text{CO})_4\}]$ and $\{[\text{PhCH}_2\text{NMe}_3]\{(\mu\text{-H})\text{Fe}_2(\text{CO})_6\text{Bi}_2(\mu\text{-Cl})_2\}\}_\infty$ and Stabilization of Reduced-Hypervalent Bismuth Centers by Coordination to a Metal Center in $[\text{PhCH}_2\text{NMe}_3]_3[\text{Bi}_3\text{Cl}_4(\mu\text{-Cl})_4\{\text{Fe}(\text{CO})_3\}]$

Jeffrey R. Eveland,[†] Jean-Yves Saillard,^{*,‡} and Kenton H. Whitmire^{*,†}

Department of Chemistry, Rice University, 6100 Main Street, Houston, Texas 77005-1892, and LCSIM-UMR C6511, Université de Rennes 1, 35042 Rennes-Cedex, France

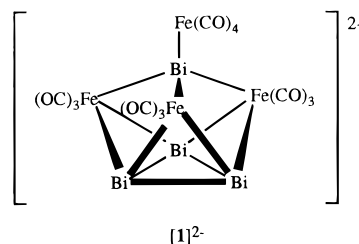
Received August 8, 1996[⊗]

The reaction of $[\text{Q}]_2[\text{Bi}_4\text{Fe}_4(\text{CO})_{13}]$ ($[\text{Q}]_2[\mathbf{1}]$; $[\text{Q}] = [\text{Et}_4\text{N}]^+$, $[\text{PhCH}_2\text{NMe}_3]^+$) with MePCl_2 in MeCN is a complicated reaction which gives different results depending upon the stoichiometry of the reaction. At a ratio of 1:1.33 (cluster:phosphine), the reaction yields a mixture of the new bismuth–iron carbonyl compounds $[\text{Q}][(\mu\text{-H})\text{Fe}_2(\text{CO})_6\text{Bi}_2\{\text{Fe}(\text{CO})_4\}]$ ($[\text{Q}][\mathbf{2}]$), which has a tetrahedral Fe_2Bi_2 core edge-bridged across the bismuth centers by an $[\text{Fe}(\text{CO})_4]^{2-}$ fragment, and $[\text{Q}]_3[\text{Bi}_3\text{Cl}_4(\mu\text{-Cl})_4\{\text{Fe}(\text{CO})_3\}]$ ($[\text{Q}]_3[\mathbf{3}]$), containing a reduced complex ion $[\text{Bi}_3\text{Cl}_8]^-$ stabilized by coordination to an iron tricarbonyl fragment. Extended Hückel molecular orbital calculations on this unusual anion are consistent with each bismuth atom possessing the same reduced oxidation state of +2.33. The compound $[\text{Et}_4\text{N}][\mathbf{2}]$ crystallizes in the triclinic space group $P\bar{1}$ (No. 2) with $a = 10.246(2)$ Å, $b = 11.859(2)$ Å, $c = 12.474(2)$ Å, $\alpha = 71.11(3)^\circ$, $\beta = 79.60(3)^\circ$, $\gamma = 76.37(3)^\circ$, $V = 1384.7(4)$ Å³, and $Z = 2$, while $[\text{PhCH}_2\text{NMe}_3]_3[\mathbf{3}] \cdot 0.87\text{Et}_2\text{O}$ was characterized in the orthorhombic space group $Pbca$ (No. 61) with $a = 20.801(4)$ Å, $b = 19.937(4)$ Å, $c = 25.480(5)$ Å, $V = 10566.8(36)$ Å³, and $Z = 8$. When the reaction is carried out at a ratio of 1:2, the novel hydride $\{[\text{Q}]\{(\mu\text{-H})\text{Fe}_2(\text{CO})_6\text{Bi}_2(\mu\text{-Cl})_2\}\}_\infty$ ($\{[\text{Q}]\{\mathbf{4}\}\}_\infty$) is isolated. This cluster also has a “tetrahedral” core, with the Bi–Bi vector bridged by a chloride ligand and the molecules joined into infinite polymeric chains in the solid state by the second intermolecularly-bridging chloride ligand. $\{[\text{PhCH}_2\text{NMe}_3]\{\mathbf{4}\}\}_\infty$ crystallizes in the monoclinic space group $P2_1/n$ (No. 14) with $a = 7.864(2)$ Å, $b = 22.465(4)$ Å, $c = 13.797(3)$ Å, $\beta = 105.96(3)^\circ$, $V = 2343.5(9)$ Å³, and $Z = 4$. The metal framework of $[\mathbf{4}]^-$ is similar to that of $[\mathbf{2}]^-$ with the notable exception that the Bi–Bi bond present in $[\mathbf{2}]^-$ is missing in $[\mathbf{4}]^-$ because of the additional electrons provided by the chloride ions. At stoichiometries greater than 2:1, the previously reported $[\text{Fe}(\text{CO})_4\text{Bi}_2\text{Cl}_6]^{2-}$ ion is formed.

Introduction

In the last decade, a great deal of attention has been given to complexes and clusters of transition metal carbonyls with main group elements.^{1–5} The reactivity of the metal clusters is profoundly influenced by the presence of main group elements as vertex atoms. Compounds containing the heavy group 15 element bismuth have received particular attention for a variety of reasons, among which is its large size. In initial studies on bismuth-containing transition metal carbonyl complexes, primarily open-framework systems such as $\text{Bi}\{\text{Co}(\text{CO})_4\}_3$ were produced, and it was thought that *closo* clusters would not form because of the steric bulk of Bi.⁷ It was later found that a wide variety of *closo* systems of bismuth with first-row transition metal carbonyls such as $\text{BiCo}_3(\text{CO})_9$,^{8,9} $[\text{BiFe}_3(\text{CO})_{10}]^-$,¹⁰ $\text{Bi}_2\text{Fe}_3(\text{CO})_9$,¹¹ and $\text{Cp}_3\text{Fe}_3(\text{CO})_3\text{Bi}$ ¹² could be synthesized, and these were in fact remarkably stable. The production of these

cluster molecules served to open synthetic pathways for larger cluster systems with very interesting structures and reactivity patterns. A cluster of particular interest is $[\text{Bi}_4\text{Fe}_4(\text{CO})_{13}]^{2-}$ ($[\mathbf{1}]^{2-}$)^{13,14} which has a novel cage structure reminiscent of Zintl



anions such as E_7^{3-} ($\text{E} = \text{P}, \text{As}, \text{Sb}$) with some vertices replaced by transition metal fragments.^{15–17} In order to understand the

[†] Rice University.

[‡] Université de Rennes 1.

[⊗] Abstract published in *Advance ACS Abstracts*, August 15, 1997.

- (1) Scheer, M.; Herrmann, E. *Z. Chem.* **1990**, *30*, 41.
- (2) Whitmire, K. H. *J. Coord. Chem.* **1988**, *17*, 95.
- (3) Norman, N. C. *Chem. Soc. Rev.* **1988**, *17*, 269.
- (4) Compton, N. A.; Errington, J.; Norman, N. C. *Adv. Organomet. Chem.* **1990**, *31*, 91.
- (5) Whitmire, K. H. *Clusters of Metals and Nonmetals*; Elsevier: Amsterdam, 1989; p 503.
- (6) Etzrodt, G.; Boese, R.; Schmid, G. *Chem. Ber.* **1979**, *112*, 2574.
- (7) Schmid, G. *Angew. Chem., Int. Ed. Engl.* **1978**, *17*, 392; *Angew. Chem.* **1978**, *90*, 417.

- (8) Whitmire, K. H.; Leigh, J. S.; Gross, M. E. *J. Chem. Soc., Chem. Commun.* **1987**, 926.
- (9) Martinengo, S.; Ciani, G. *J. Chem. Soc., Chem. Commun.* **1987**, 1589.
- (10) Whitmire, K. H.; Lagrone, C. B.; Churchill, M. R.; Fettinger, J. C.; Biondi, L. V. *Inorg. Chem.* **1984**, *23*, 4227.
- (11) Churchill, M. R.; Fettinger, J. C.; Whitmire, K. H. *J. Organomet. Chem.* **1985**, *284*, 13.
- (12) Wallis, J. M.; Müller, G.; Riede, J.; Schmidbaur, H. *J. Organomet. Chem.* **1989**, *369*, 165.
- (13) Whitmire, K. H.; Churchill, M. R.; Fettinger, J. C. *J. Am. Chem. Soc.* **1985**, *107*, 1056.
- (14) Whitmire, K. H.; Albright, T. A.; Kang, A.-K.; Churchill, M. R.; Fettinger, J. C. *Inorg. Chem.* **1986**, *25*, 2799.

chemistry of this intriguing cluster, we have begun to probe its reactivity with a variety of reagents. In particular, we were interested in determining if the open Bi_3 face could be capped by an additional fragment. In the reaction with MePCl_2 , the metal-containing products obtained were found to be quite different from those anticipated, were dependent upon the stoichiometry of the reaction, and did not incorporate phosphorus. This work reports the isolation and structural/spectroscopic characterization of $[\text{Et}_4\text{N}][(\mu\text{-H})\text{Fe}_2(\text{CO})_6\text{Bi}_2\{\text{Fe}(\text{CO})_4\}]$ ($[\text{Et}_4\text{N}][\mathbf{2}]$), $[\text{PhCH}_2\text{NMe}_3]_3[\text{Bi}_3\text{Cl}_4(\mu\text{-Cl})_4\text{Fe}(\text{CO})_3]$ ($[\text{PhCH}_2\text{NMe}_3][\mathbf{3}]$) and $[\text{PhCH}_2\text{NMe}_3][(\mu\text{-H})\text{Fe}_2(\text{CO})_6\text{Bi}_2\{\mu\text{-Cl}\}_2]$ ($[\text{PhCH}_2\text{NMe}_3][\mathbf{4}]$), which arise from reactions of salts of $[\mathbf{1}]^{2-}$ with MePCl_2 .

Experimental Section

General Considerations. All reactions were performed under an inert atmosphere of nitrogen or argon using standard Schlenk/vacuum-line techniques. Diethyl ether and tetrahydrofuran were dried by distillation from CaH_2 followed by distillation from $\text{Na/Ph}_2\text{CO}$ ketyl. Acetonitrile was distilled from CaH_2 prior to use. Infrared spectra were obtained with a Perkin-Elmer Model 1640 FTIR instrument, and ^1H (250.13 MHz) and $^{13}\text{C}\{^1\text{H}\}$ (62.90 MHz) NMR spectra were measured on a Bruker AC 250 spectrometer in the solvent noted. Analyses for carbon monoxide content were performed by digestion of the compound with $[\text{PyH}]\text{Br}_3$ in degassed CH_2Cl_2 at 75°C in a vacuum flask, followed by quantitation of the liberated CO using a Toepler pump. The $[\text{Q}]_2\text{-}[\text{Bi}_4\text{Fe}_4(\text{CO})_{13}]$ complexes were prepared by the literature methods.^{13,14} Methylchlorophosphine was used as received from Strem Chemicals.

Synthesis of $[\text{Q}][\mathbf{2}]$ and $[\text{Q}][\mathbf{3}]$ from $[\text{Q}][\mathbf{1}]$ and MePCl_2 (1:1.33). In these preparations the $[\text{Et}_4\text{N}]^+$ and $[\text{PhCH}_2\text{NMe}_3]^+$ ions perform chemically the same, but the X-ray crystallography was complicated for one or the other because of disorder of the cation or problems in crystallization. Approximately 50 mL of MeCN was added to a 100 mL Schlenk flask containing $[\text{PhCH}_2\text{NMe}_3]_2[\mathbf{1}]$ (1.01 g 0.586 mmol). MePCl_2 (1.33 equiv, 0.09 g, 0.07 mL) was then added via syringe to the solution, upon which the red-brown color of the initial solution changed slightly to a deeper red. The resulting solution was allowed to stir for 1 h under argon, after which it was filtered through a glass frit and the solvent was removed *in vacuo*. The residue was extracted with several portions of Et_2O to remove the phosphorus-containing byproducts. The dark solid was then extracted with a few 20 mL portions of THF, and the combined deep red-brown filtrates were concentrated to 15 mL, layered with hexanes, and allowed to stand for 2–3 days at 0°C , during which large columnar crystals of $[\text{PhCH}_2\text{NMe}_3][\mathbf{2}]$ appeared. Yield: 0.51 g (65% based upon Fe). The synthesis of the $[\text{Et}_4\text{N}]^+$ salt was performed in a similar manner using $[\text{Et}_4\text{N}]_2[\mathbf{1}]$ in place of $[\text{PhCH}_2\text{NMe}_3]_2[\mathbf{1}]$. The spectroscopic data for both salts are essentially identical, and the values reported here are those of the $[\text{Et}_4\text{N}]^+$ salt. IR (ν_{CO} , cm^{-1} ; THF): 2033 (vw), 1992 (s), 1985 (s), 1934 (br, m). ^1H NMR (CD_3CN , ppm): $\delta = 3.15$ (q, CH_2), 1.20 (t, CH_3) -14.74 (s, $\mu\text{-H}$). $^{13}\text{C}\{^1\text{H}\}$ NMR (THF- d_8 , 0.5 wt % $\text{Cr}[\text{MeC}(\text{O})\text{CHC}(\text{O})\text{Me}]_3$ added as a relaxation agent, 295 K, ppm): $\delta = 212.4$ (s, CO), 211.0 (s, CO), 210.3 (s, CO) 209.4 (s, CO), 53.1 (s, CH_3CH_2 of Et_4N^+), 7.5 (s, (CH_3CH_2) of Et_4N^+). Anal. Calcd (found): CO, 0.88 mmol/g (0.87 mmol/g). $[\text{Et}_4\text{N}][\mathbf{2}]$ is soluble in MeCN, acetone, CH_2Cl_2 , and THF but insoluble in Et_2O and hexanes.

The solid remaining after the THF extraction was further extracted with MeCN (2×20 mL). The filtrates were combined and filtered through diatomaceous earth. After the solvent was removed *in vacuo*, the solid was washed with two portions each of THF and Et_2O . The remaining red-orange solid was dried thoroughly under vacuum to yield pure $[\text{PhCH}_2\text{NMe}_3][\mathbf{3}]$. The compound was recrystallized at 0°C by layering a concentrated MeCN solution of the product with Et_2O . After 1–2 days, small block-shaped light orange crystals of $[\text{PhCH}_2\text{NMe}_3]_3\text{-}[\mathbf{3}] \cdot 0.87\text{Et}_2\text{O}$ had formed. This compound was recrystallized by

layering a concentrated solution of it in MeCN with Et_2O . Crystals appeared upon standing at 0°C for a few of days. Yield: 0.24 g (21% based upon Bi). IR (ν_{CO} , cm^{-1} ; MeCN): 2029 (w), 1980 (vs). ^1H NMR (CD_3CN , ppm): $\delta = 7.48$ (m, C_6H_5), 7.26 (m, C_6H_5), 3.97 (s, CH_2), 1.94 (s, NMe_3). ^{13}C NMR [^1H] (0.5 wt % $\text{Cr}[\text{MeC}(\text{O})\text{CHC}(\text{O})\text{Me}]_3$ added as a relaxation agent, 295 K, ppm): $\delta = 217.3$ (s, CO), 136.3, 131.6, 130.2, 128.1 (s, C_6H_5), 75.1 (s, CH_2), 58.2 (t, NMe_3). Anal. Calcd (found): CO, 0.97 mmol/g (0.95 mmol/g). $[\text{PhCH}_2\text{NMe}_3][\mathbf{3}]$ is soluble in MeCN, slightly soluble in acetone, but insoluble in CH_2Cl_2 , THF, Et_2O , and hexanes.

Synthesis of $[\text{Q}][\mathbf{4}]$ from $[\text{Q}][\mathbf{1}]$ and MePCl_2 . A 50 mL portion of MeCN was added to a 100 mL Schlenk flask containing $[\text{PhCH}_2\text{NMe}_3]_2[\mathbf{1}]$ (0.509 g, 0.295 mmol); 2.0 equiv of MePCl_2 (0.07 g, 0.05 mL) was then added via syringe. The solution became deep red and was allowed to stir for approximately 10 h, during which it became dark green. The mixture was then filtered through diatomaceous earth, and the solvent was removed under vacuum. The resulting dark green oil was washed with several 50 mL portions of Et_2O , and the residue was placed in a Soxhlet extraction thimble and extracted with additional Et_2O for a few hours to remove the residual phosphine byproducts. The remaining dark green solid was extracted with a few 20 mL portions of THF, and the combined dark green filtrates were concentrated to ca. 15 mL. The solution was layered with hexanes and allowed to stand for about 3 days at 0°C , giving dark green needlelike crystals of $[\text{PhCH}_2\text{NMe}_3][\mathbf{4}]$. Yield: 0.27 g (49% based upon Bi or Fe). IR (ν_{CO} , cm^{-1} ; THF): 2025 (m), 1997 (s), 1956 (m, sh), 1943 (ms). ^1H NMR (CD_3CN , ppm): $\delta = 7.50$ (m, C_6H_5), 7.28 (m, C_6H_5), 3.98 (s, CH_2), 1.93 (s, NMe_3), -17.67 (s, $\mu\text{-H}$). ^{13}C NMR (THF- d_8 , 0.5 wt % $\text{Cr}[\text{MeC}(\text{O})\text{CHC}(\text{O})\text{Me}]_3$ added as a relaxation agent, 295 K, ppm): $\delta = 215.6$ (s, CO), 195.5 (s, CO), 134.1, 131.6, 130.1, 129.3 (s, C_6H_5), 71.5 (s, CH_2), 53.4 (t, NMe_3). Anal. Calcd (found): CO, 1.08 mmol/g (1.06 mmol/g). $[\text{PhCH}_2\text{NMe}_3][\mathbf{4}]$ is soluble in MeCN and THF, very slightly soluble in CH_2Cl_2 and acetone, but insoluble in Et_2O and hexanes.

Isolation and Characterization of Phosphine Byproducts. The Et_2O fractions from the Soxhlet extraction described above for the synthesis of salts of $[\mathbf{4}]^-$ were combined, and the solvent was removed under vacuum. The colorless oil obtained was then distilled at room temperature and a pressure of $0.1 \mu\text{m}$ to give a less viscous fraction (fraction 1) and a very thick residue (fraction 2). These fractions were then used for the spectral analyses.

(a) Fraction 1. IR (cm^{-1} , neat on KBr): 2087 (br, m), 1653 (s), 1419 (w). ^1H NMR (THF- d_8 , 293 K, ppm): $\delta = 8.22$ (s), 6.06 (s), 5.92 (m), 5.08 (s), 4.84 (dd), 3.98 (d), 3.62 (t), 1.78 (p), 1.44 (t), 1.38 (s), 0.88 (m), 0.83 (m). ^{31}P NMR (THF- d_8 , 293 K, ppm): $\delta = 45.01$ (s), 44.35 (br), 37.59 (s). $^{31}\text{P}\{^1\text{H}\}$ NMR (THF- d_8 , 293 K, ppm): 44.42 (d, $^1J_{\text{C-H}} = 533$ Hz), 37.59 (s).

(b) Fraction 2. IR (cm^{-1} , neat on KBr): 2385 (m), 1718 (m, sh), 1643 (br, m), 1417 (w), 1305 (m), 1260 (m) 1102 (s, br), 1017 (s), 950 (m, sh), 846 (m), 798 (m), 737 (w). ^1H NMR ($\text{C}_4\text{D}_8\text{O}$, 293 K, ppm): $\delta = 11.62$ (s), 7.68 (m), 7.54 (mult), 5.90 (mult), 5.27 (sept), 5.18 (t), 5.03 (d), 4.48 (br), 4.21 (s), 1.29 (s), 0.89 (mult). ^{31}P NMR ($\text{C}_4\text{D}_8\text{O}$, 293 K, ppm): 43.57 (s), 36.86 (br); decoupling hydrogen had no effect on the spectrum.

The mass spectrum (CI^+) of fraction 1 showed the highest mass (M^+) at m/e 1117 and a regular loss of groups with m/e 74–75 down to m/e 523, below which there was no obvious pattern. The species were present in larger percentages as the mass decreased. Similarly, the mass spectrum of fraction 2 (CI^+) showed the highest mass at m/e 1113 and a regular loss of groups with m/e 74–75 down to m/e 207, below which there was no obvious pattern. As with fraction 1, as the mass decreased the relative amount increased. In both cases, the masses appeared in two groups separated by 15–16 mass units, which is attributable to the use of CH_4 as the carrier gas for the CI experiment. There was an intensity difference in these two groupings, however, between fractions 1 and 2. For fraction 1, the two groupings had roughly the same intensity, while, for fraction 2, the intensity of the lighter series was about twice that of the heavier set.

These phosphine compounds are soluble in MeCN, acetone, and THF, slightly soluble in Et_2O , but insoluble in hexanes.

X-ray Crystal Structure Determinations of $[\text{Et}_4\text{N}][\mathbf{2}]$, $[\text{PhCH}_2\text{NMe}_3][\mathbf{3}]$, and $[\text{PhCH}_2\text{NMe}_3][\mathbf{4}]$. All crystallographic data

(15) Adolphson, D. G.; Corbett, J. D.; Merryman, D. J. *J. Am. Chem. Soc.* **1976**, *98*, 7234.

(16) Schmettow, W.; von Schnering, H. G. *Angew. Chem.* **1977**, *89*, 895; *Angew. Chem., Int. Ed. Engl.* **1977**, *16*, 857.

(17) Critchlow, S. C.; Corbett, J. D. *Inorg. Chem.* **1984**, *23*, 770.

Table 1. Crystal Data and Crystallographic Data Collection and Structure Refinement Parameters for [Et₄N][2], [PhCH₂NMe₃]₃[3]·0.87Et₂O, and [{PhCH₂NMe₃}]₃[4]_∞

	[Et ₄ N][2]	[PhCH ₂ NMe ₃] ₃ [3]·0.87Et ₂ O	[{PhCH ₂ NMe ₃ }] ₃ [4] _∞
empirical formula	C ₁₈ H ₂₁ Bi ₂ Fe ₃ NO ₁₀	C ₃₃ H ₄₈ Bi ₃ Cl ₈ FeN ₃ O ₃ ·0.87C ₄ H ₁₀ O	C ₁₆ H ₁₇ Bi ₂ Cl ₂ Fe ₂ NO ₆
fw	996.87	1564.88	919.87
temp (K)	293(2)	293(2)	223(2)
system [space group]	triclinic [$P\bar{1}$ (No. 2)]	orthorhombic [$Pbca$ (No. 61)]	monoclinic [$P2_1/n$ (No. 14)]
cell parameters			
<i>a</i> (Å)	10.246(2)	20.801(4)	7.864(2)
<i>b</i> (Å)	11.859(2)	19.937(4)	22.465(4)
<i>c</i> (Å)	12.474(2)	25.480(5)	13.797(3)
α (deg)	71.11(3)		
β (deg)	79.60(3)		105.96(3)
γ (deg)	76.37(3)		
<i>V</i> (Å ³)	1384.7(4)	10 566.8(36)	2343.5(9)
<i>Z</i>	2	4	4
ρ_{calc} (g/cm ³)	2.391	1.967	2.604
μ (mm ⁻¹)	14.247	10.671	16.445
goodness of fit (on <i>F</i> ²)	1.021	1.022	1.027
final <i>R</i> [<i>I</i> > 2 σ (<i>I</i>)]			
<i>R</i> ₁ ^a (on <i>F</i>)	0.0397	0.0691	0.0286
<i>wR</i> ₂ ^a (on <i>F</i> ²)	0.0711	0.1417	0.0564
final <i>R</i> (all data)			
<i>R</i> ₁ ^a (on <i>F</i>)	0.1070	0.1979	0.0560
<i>wR</i> ₂ ^a (on <i>F</i> ²)	0.0879	0.1894	0.0639

$$^a R_1 = \sum ||F_o| - |F_c|| / \sum |F_o|; wR_2 = [\sum w(F_o^2 - F_c^2)^2 / \sum wF_o^4]^{1/2}; w^{-1} = \sigma^2(F_o^2) + aP^2 + bP; P = (F_o^2 + 2F_c^2)/3.$$

were measured with a Rigaku AFC5S four-circle automated diffractometer (Rigaku CONTROL Automatic Data Collection Series, Molecular Structure Corp., The Woodlands, TX) using graphite monochromated Mo K α radiation (0.7107 Å). A summary of data collection parameters for the three compounds is given in Table 1. The crystals were mounted on a glass fiber with epoxy cement, and data were collected with 2θ - ω scans at 4°/min. Three standard reflections were monitored for decay every 150 reflections throughout the data collection. An absorption correction from azimuthal (ψ) scans was applied to the data. The programs used in solving each structure were part of the Siemens Analytical X-Ray Instruments data reduction and refinement package SHELXTL PC,¹⁸ and refinement of each structure was performed using the data refinement program package SHELXL-93.¹⁹

A dark, columnar crystal of [Et₄N][2] (0.3 × 0.3 × 0.5 mm³) grown as described above was used for data collection and found to be triclinic. Data were collected for $+h, \pm k, \pm l$ over the ranges $0 \leq h \leq 13, -15 \leq k \leq 15, -16 \leq l \leq 16$ with $2\theta_{\text{max}} = 55^\circ$. The more common centrosymmetric space group $P\bar{1}$ (No. 2) was chosen on the basis of reflection intensity statistics and its natural occurrence and shown to be correct by successful structure solution and refinement. The bismuth, iron, carbon, and oxygen atoms of the anion and the nitrogen atom of the counterion were refined anisotropically, while the non-hydrogen atoms of the cation and the cluster-bound hydride ligand were refined isotropically. All hydrogen atoms of the cation were included in calculated positions, while the hydride ligand attached to the cluster was located and refined isotropically.

The crystal (0.3 × 0.3 × 0.3 mm³) of [PhCH₂NMe₃]₃[3]·0.87Et₂O chosen for study was grown from Et₂O/MeCN as described above. Data were collected for $+h, +k, +l$ over the ranges $0 \leq h \leq 20, 0 \leq k \leq 20, -21 \leq l \leq 0$ with $2\theta_{\text{max}} = 45^\circ$. The centrosymmetric space group $Pbca$ (No. 61) was chosen on the basis of systematic absences and intensity statistics. The phenyl rings of the cations were restrained to refine as rigid bodies. Because of the weighting of the data by the large number of heavy atoms, bond parameters to the carbon atoms of the carbonyl ligands were outside of normal ranges, so the Fe–C and C–O distances were also restrained in the final refinement. The bismuth, iron, and oxygen atoms of the anion and all non-hydrogen atoms of the cations were refined anisotropically. The remaining carbon atoms in the anion were refined isotropically. The largest peak in the final difference map was 2.28 e/Å³ and was a shadow of the bismuth atom.

Crystals of [{PhCH₂NMe₃}]₃[4]_∞ suitable for single-crystal X-ray diffraction were grown by vapor phase diffusion of hexanes into a concentrated solution of the compound in THF at 0 °C. A dark green needlelike crystal (0.2 × 0.3 × 0.5 mm³) was chosen for data collection, and the starting cell was determined to be monoclinic. The centrosymmetric space group $P2_1/n$ (No. 14) was selected on the basis of systematic absences and intensity statistics. All non-hydrogen atoms were refined anisotropically. The bridging hydride ligand of the anion was refined isotropically. Hydrogen atoms on the cation were included in calculated positions.

Computational Details. Calculations on [3]³⁻ were carried out within the standard extended Hückel (EH) formalism^{20,21} using the modified Wolfsberg–Helmholz formula.²² The calculations were carried out with the CACAO package developed by Mealli and Proserpio.²³ Standard atomic parameters were used for C and O.²¹ Parameters for Cl,²⁴ Bi,²⁵ and Fe²⁵ were taken from the literature. It has been confirmed that a reasonable variation of the atomic Bi, Cl, and Fe *H_{ii}* parameters do not modify significantly the qualitative conclusions of this study. Calculations were run both on the experimental structure and on an averaged idealized geometry of C_{2v} symmetry, which would be an exact symmetry if the slight variations in Bi–Cl and Fe–CO bond parameters were ignored (see below).

Results and Discussion

Syntheses. The reaction of tetraalkylammonium salts of [1]²⁻ with MePCl₂ in MeCN at a ratio of 1:1.3 yields two main products, [2]⁻ and [3]³⁻, along with small amounts of metallic residues and polymeric phosphine-containing byproducts. Note: To facilitate discussion, the counterions have been omitted and the compounds will be referred to by the anion only. In all cases, the cations were either [Et₄N]⁺ or [PhCH₂NMe₃]⁺ and the chemistry did not seem to depend upon which was chosen. The crystallography, however, was sometimes cation dependent, and the sample chosen was selected in order to overcome problems in the cation for the other salt. For example, we were unable to obtain single crystals of [PhCH₂NMe₃][2],

(20) Hoffmann, R. *J. Chem. Phys.* **1963**, *39*, 1397.

(21) Hoffmann, R.; Lipscomb, W. N. *J. Chem. Phys.* **1962**, *36*, 2179.

(22) Ammeter, J. H.; Bürgi, H.-B.; Thibeault, J. C.; Hoffmann, R. *J. Am. Chem. Soc.* **1978**, *100*, 3686.

(23) Mealli, C.; Proserpio, D. M. *J. Chem. Educ.* **1990**, *67*, 399.

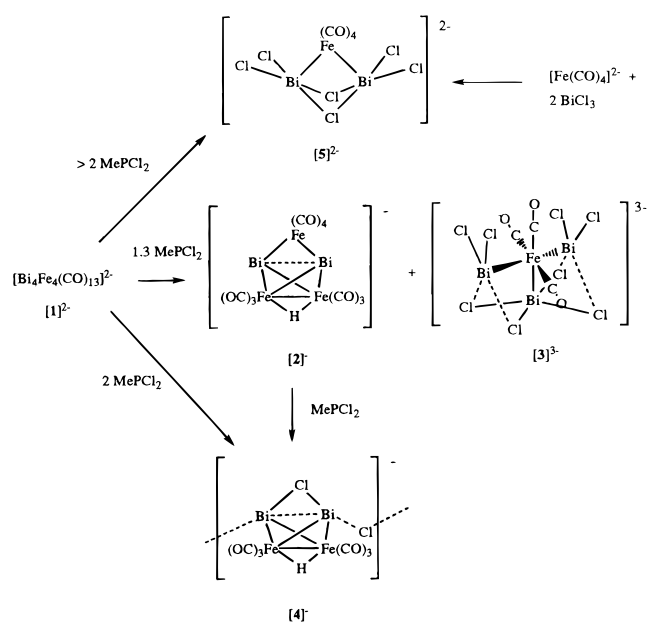
(24) Summerville, R. H.; Hoffmann, R. *J. Am. Chem. Soc.* **1976**, *98*, 7240.

(25) Kahlal, S.; Halet, J.-F.; Saillard, J.-Y.; Whitmire, K. H. *J. Organomet. Chem.* **1994**, *478*, 1.

(18) Sheldrick, G. M. *SHELXTL PC*; Siemens Analytical X-Ray Instruments, Inc.: Madison, WI, 1990.

(19) Sheldrick, G. M. *SHELXL-93*; In University of Göttingen: Göttingen, Germany, 1993.

Scheme 1



so the $[\text{Et}_4\text{N}]^+$ salt was structurally characterized instead. The reaction is rapid with approximately 80% of the starting carbonyl compound being converted within 15–20 min. $[\mathbf{4}]^-$ is obtained via the same reaction but at a stoichiometric ratio of one cluster to two MePCl_2 . Several hours are required for completion of this reaction. When greater than 2 equiv of MePCl_2 is used, the major isolated product is $[\text{Bi}_2\text{Cl}_6\text{Fe}(\text{CO})_4]^{2-}$, whose characterization has been reported.²⁶ This compound may also be obtained directly by reaction of two equiv of BiCl_3 with $[\text{Fe}(\text{CO})_4]^{2-}$. These reactions are summarized in Scheme 1. Salts of $[\mathbf{2}]^-$ and $[\mathbf{3}]^{3-}$ may be isolated from the reaction using a 1:2 stoichiometry if the reaction is quenched by addition of Et_2O prior to the formation of $[\mathbf{4}]^-$. As will be discussed below, the anions $[\mathbf{2}]^-$ and $[\mathbf{4}]^-$ are structurally related and $[\mathbf{4}]^-$ is derived from $[\mathbf{2}]^-$ upon addition of MePCl_2 but the fate of $[\mathbf{3}]^{3-}$ under such conditions is unknown. Significant amounts of insoluble and non-carbonyl-containing residues result from the second reaction, so $[\mathbf{3}]^{3-}$ apparently undergoes decomposition.

The differing solubilities of $[\mathbf{2}]^-$ and $[\mathbf{3}]^{3-}$ allow their easy separation. The monoanionic $[\mathbf{2}]^-$ is soluble in THF, CH_2Cl_2 , and MeCN and somewhat soluble in acetone, although the compound is not very stable in MeCN solution, decomposing over a period of several hours to 1 day. Compound $[\mathbf{3}]^{3-}$, on the other hand, because of its high charge is soluble only in MeCN. Compound $[\mathbf{4}]^-$ dissolves readily in MeCN and THF but not in CH_2Cl_2 . The latter insolubility makes separation of mixtures of $[\mathbf{2}]^-$ and $[\mathbf{4}]^-$ facile (the solubilities of the $[\text{Et}_4\text{N}]^+$ and $[\text{PhCH}_2\text{NMe}_3]^+$ salts were very similar). Compound $[\mathbf{4}]^-$ is more unstable in MeCN solution, with complete decomposition occurring in 2–3 h. Both $[\mathbf{2}]^-$ and $[\mathbf{4}]^-$ are only moderately air sensitive in the solid state as the tetraalkylammonium salts.

Structure and Bonding Considerations. Thermal ellipsoid plots of the cluster anions $[\mathbf{2}]^-$, $[\mathbf{3}]^{3-}$, and $[\mathbf{4}]^-$ are given in Figures 1–4, and selected bond parameters are provided in Tables 2–4. Since the anions $[\mathbf{2}]^-$ (Figure 1) and $[\mathbf{4}]^-$ (Figures 3 and 4) are structurally related, they will be discussed together. Both compounds are monoanionic with one counteranion present in the crystal lattice, and both may be derived by starting with a Bi_2Fe_2 tetrahedral core. The parent is the as-yet-unknown tetrahedral dianion $[\text{Bi}_2\text{Fe}_2(\text{CO})_6]^{2-}$, possessing six skeletal

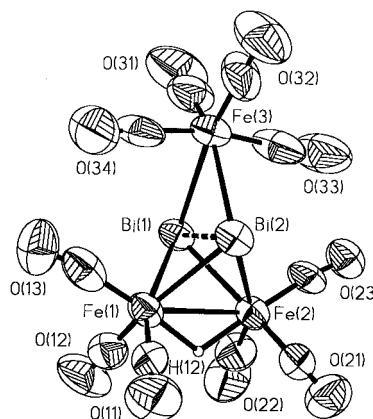


Figure 1. Plot of the anion of $[\text{Et}_4\text{N}][\mathbf{2}]$ showing 50% thermal ellipsoids and the atom-labeling scheme.

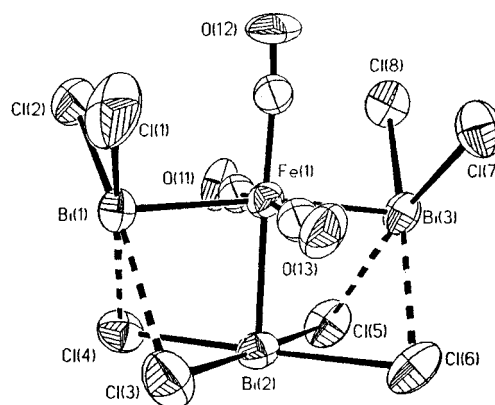


Figure 2. Plot of the anion of $[\text{PhCH}_2\text{NMe}_3][\mathbf{3}] \cdot 0.87\text{Et}_2\text{O}$ showing 50% thermal ellipsoids and the atom-labeling scheme.

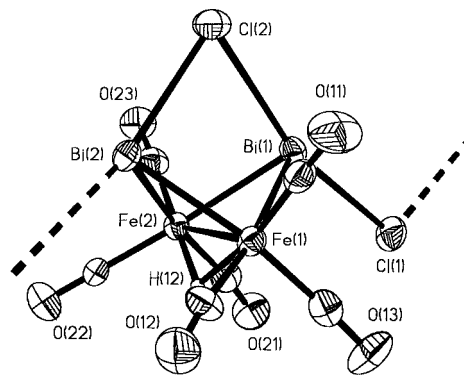


Figure 3. Plot of the anion of $[\{\text{PhCH}_2\text{NMe}_3\}\{\mathbf{4}\}]_\infty$ showing 50% thermal ellipsoids and the atom-labeling scheme.

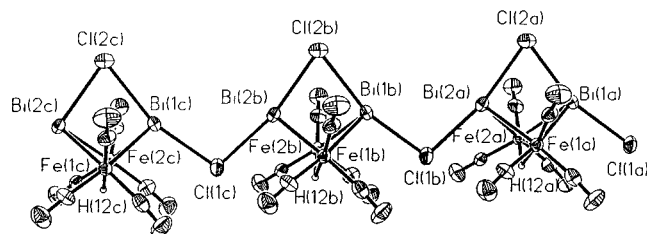


Figure 4. Plot of a portion of the polymeric chain structure found in the solid state for $[\{\text{PhCH}_2\text{NMe}_3\}\{\mathbf{4}\}]_\infty$.

electron pairs for edge-localized bonding within the tetrahedron. Protonation of this structure across the Fe–Fe edge results in no change to the electron count or the core structure except for a lengthening of the metal–metal bond. The Fe–Fe bond distances are the same for $[\mathbf{2}]^-$ and $[\mathbf{4}]^-$ within experimental error (2.753(4) and 2.759(2) Å, respectively) and are consistent

(26) Eveland, J. R.; Whitmire, K. H.; Saillard, J.-Y. *Inorg. Chem.* **1996**, *35*, 4400–4405.

Table 2. Selected Bond Distances (Å) and Angles (deg) for [Et₄N][2]

Distances			
Bi(1)–Bi(2)	3.102(1)	Bi(1)–Fe(1)	2.701(3)
Bi(1)–Fe(2)	2.702(2)	Bi(1)–Fe(3)	2.896(3)
Bi(2)–Fe(1)	2.695(3)	Bi(2)–Fe(2)	2.705(2)
Bi(2)–Fe(3)	2.882(3)	Fe(1)–Fe(2)	2.753(4)
Fe(1)–H(12)	1.74(11)	Fe(2)–H(12)	1.60(13)
Bi(2)···Bi(2A) ^a	3.610(2)		
Angles			
Fe(1)–Bi(1)–Fe(2)	61.26(8)	Fe(1)–Bi(1)–Fe(3)	103.28(8)
Fe(1)–Bi(1)–Bi(2)	54.82(6)	Fe(2)–Bi(1)–Fe(3)	103.19(8)
Fe(2)–Bi(1)–Bi(2)	55.05(6)	Fe(3)–Bi(1)–Bi(2)	57.32(5)
Fe(1)–Bi(2)–Fe(2)	61.30(8)	Fe(1)–Bi(2)–Fe(3)	103.81(8)
Fe(1)–Bi(2)–Bi(1)	55.00(6)	Fe(2)–Bi(2)–Fe(3)	103.48(8)
Fe(2)–Bi(2)–Bi(1)	54.95(5)	Fe(3)–Bi(2)–Bi(1)	57.76(5)
Bi(1)–Fe(1)–Bi(2)	70.17(7)	Bi(1)–Fe(1)–Fe(2)	59.39(7)
Bi(2)–Fe(1)–Fe(2)	59.54(8)	Bi(1)–Fe(2)–Bi(2)	70.00(7)
Bi(1)–Fe(2)–Fe(1)	59.35(7)	Bi(2)–Fe(2)–Fe(1)	59.17(8)
Bi(1)–Fe(3)–Bi(2)	64.92(6)		

^a Symmetry transformation used to generate the equivalent atom Bi(2A): $-x + 1, -y + 1, -z + 1$.

Table 3. Selected Bond Distances (Å) and Angles (deg) for [PhCH₂NMe₃]₃[3]·0.87Et₂O

Distances			
Bi(1)–Fe(1)	2.602(4)	Bi(2)–Fe(1)	2.646(4)
Bi(3)–Fe(1)	2.612(4)	Bi(1)–Cl(1)	2.594(11)
Bi(1)–Cl(2)	2.610(8)	Bi(1)–Cl(3)	3.094(9)
Bi(1)–Cl(4)	3.154(10)	Bi(2)–Cl(3)	2.814(10)
Bi(2)–Cl(4)	2.763(8)	Bi(2)–Cl(5)	2.775(9)
Bi(2)–Cl(6)	2.838(9)	Bi(3)–Cl(5)	3.125(9)
Bi(3)–Cl(6)	2.964(8)	Bi(3)–Cl(7)	2.598(9)
Bi(3)–Cl(8)	2.662(8)	Fe–C (range)	1.80(3)–1.83(3)
C–O (range)	1.12(3)–1.14(3)		
Angles			
Cl(2)–Bi(1)–Cl(1)	92.9(3)	Cl(3)–Bi(1)–Cl(1)	98.5(3)
Cl(4)–Bi(1)–Cl(1)	171.5(3)	Cl(3)–Bi(1)–Cl(2)	168.4(3)
Cl(4)–Bi(1)–Cl(2)	95.2(3)	Cl(4)–Bi(1)–Cl(3)	73.3(2)
Cl(1)–Bi(1)–Fe(1)	98.2(3)	Cl(2)–Bi(1)–Fe(1)	97.2(2)
Cl(3)–Bi(1)–Fe(1)	83.6(2)	Cl(4)–Bi(1)–Fe(1)	83.5(2)
Cl(4)–Bi(2)–Cl(3)	84.0(3)	Cl(5)–Bi(2)–Cl(3)	178.4(3)
Cl(6)–Bi(2)–Cl(3)	99.1(3)	Cl(5)–Bi(2)–Cl(4)	94.9(3)
Cl(6)–Bi(2)–Cl(4)	176.8(2)	Cl(6)–Bi(2)–Cl(5)	82.0(2)
Cl(3)–Bi(2)–Fe(1)	88.5(2)	Cl(4)–Bi(2)–Fe(1)	90.8(2)
Cl(5)–Bi(2)–Fe(1)	90.3(2)	Cl(6)–Bi(2)–Fe(1)	88.5(2)
Cl(6)–Bi(3)–Cl(5)	74.3(2)	Cl(7)–Bi(3)–Cl(5)	169.9(2)
Cl(8)–Bi(3)–Cl(5)	97.0(3)	Cl(7)–Bi(3)–Cl(6)	95.6(3)
Cl(8)–Bi(3)–Cl(6)	171.0(3)	Cl(8)–Bi(3)–Cl(7)	93.1(3)
Cl(5)–Bi(3)–Fe(1)	83.6(2)	Cl(6)–Bi(3)–Fe(1)	86.5(2)
Cl(7)–Bi(3)–Fe(1)	96.2(2)	Cl(8)–Bi(3)–Fe(1)	95.0(2)
Bi(2)–Cl(3)–Bi(1)	74.4(2)	Bi(2)–Cl(4)–Bi(1)	74.1(2)
Bi(2)–Cl(5)–Bi(3)	73.6(2)	Bi(2)–Cl(6)–Bi(3)	75.3(2)
C(11)–Fe(1)–C(12)	93.4(14)	C(11)–Fe(1)–C(13)	173.3(14)
C(12)–Fe(1)–C(13)	92.2(14)	Bi(1)–Fe(1)–Bi(2)	86.04(12)
Bi(1)–Fe(1)–Bi(3)	170.8(2)	Bi(2)–Fe(1)–Bi(3)	84.77(13)
Bi(1)–Fe(1)–C(11)	90.6(10)	Bi(1)–Fe(1)–C(12)	95.6(10)
Bi(1)–Fe(1)–C(13)	90.1(10)	Bi(2)–Fe(1)–C(11)	85.3(10)
Bi(2)–Fe(1)–C(12)	178.4(10)	Bi(2)–Fe(1)–C(13)	88.1(10)
Bi(3)–Fe(1)–C(11)	88.3(10)	Bi(3)–Fe(1)–C(12)	93.6(10)
Bi(3)–Fe(1)–C(13)	90.1(10)		

with distances found for other Fe–Fe bonds which have been elongated by the presence of a bridging hydride ligand.^{27–29} A good comparison can be made with the isostructural and

Table 4. Selected Bond Distances (Å) and Angles (deg) for [PhCH₂NMe₃]₄[4]^a

Distances			
Bi(1)–Fe(1)	2.662(2)	Bi(2)–Fe(2)	2.641(2)
Bi(1)–Fe(2)	2.653(2)	Bi(2)–Cl(1A)	2.867(3)
Bi(1)–Cl(1)	2.818(3)	Bi(2)–Cl(2)	2.867(3)
Bi(1)–Cl(2)	2.906(3)	Fe(1)–Fe(2)	2.759(2)
Bi(1)···Bi(2)	3.4620(10)	Bi(2)–Fe(1)	2.658(2)
Fe(1)–H(12)	1.83(9)	Fe(2)–H(12)	1.55(9)
Angles			
Fe(1)–Bi(1)–Fe(2)	62.54(5)	Fe(1)–Bi(2)–Bi(1)	49.45(4)
Fe(1)–Bi(1)–Cl(1)	100.37(7)	Fe(1)–Bi(2)–Fe(2)	62.75(5)
Fe(1)–Bi(1)–Cl(2)	92.63(7)	Fe(1)–Bi(2)–Cl(1A)	95.66(7)
Fe(2)–Bi(1)–Cl(1)	102.02(7)	Fe(1)–Bi(2)–Cl(2)	93.38(7)
Fe(2)–Bi(1)–Cl(2)	92.39(7)	Fe(2)–Bi(2)–Cl(1A)	98.09(7)
Cl(1)–Bi(1)–Cl(2)	163.88(8)	Cl(1B)–Bi(2)–Cl(2)	167.80(8)
Bi(1)–Fe(1)–Bi(2)	81.19(4)	Bi(1)–Fe(2)–Bi(2)	81.69(4)
Bi(1)–Fe(1)–Fe(2)	58.57(4)	Bi(1)–Fe(2)–Fe(1)	58.89(5)
Bi(2)–Fe(1)–Fe(2)	58.32(5)	Bi(2)–Fe(2)–Fe(1)	58.93(4)
Bi(1)–Cl(1)–Bi(2B)	101.56(9)	Bi(1)–Cl(2)–Bi(2)	73.56(6)

^a Symmetry transformations used to generate equivalent atoms: (A) $x + 1, y, z$; (B) $x - 1, y, z$.

isoelectronic [Et₄N][Bi₂Fe₂Co(CO)₁₀], which has no bridging hydride and an Fe–Fe bond distance of 2.682(7) Å.³⁰

The major difference between the structures of [2][−] and [4][−] lies in the effect of the group which adds across the Bi–Bi bond. From one viewpoint, the Fe(CO)₄ group considered as a 16-electron fragment does not serve to add electrons to the cluster core but rather may be viewed as accepting the electron pair present in the Bi–Bi bond to form a three-center two-electron bond. Even so, substantial Bi–Bi bonding is retained—the distance is 3.102(1) Å, consistent with a bond order of ca. 1. For comparison, the closest bonding contact in elemental Bi is 3.07 Å.³¹ Similar values have been found for clusters with bismuth–bismuth single bonds, such as Bi₉⁵⁺ in the compounds [Bi₉]₂[Bi₂Cl₈][BiCl₅]₄ (3.103(6) Å)³² and [Bi₉][Bi][HfCl₆] (3.094(3) Å),³³ as well as in [Et₄N]₂[1] (3.14(2)–3.168(2) Å)¹⁴ and [Et₄N][Bi₂Fe₂Co(CO)₁₀] (3.092(2) Å).³⁰ The bonding situation is not so simple, however. Our calculations²⁵ have shown that the interaction between the 16-electron M(CO)₄ unit and the 6-SEP *closo*-M₂Bi₂ cluster results in a significant donation from the μ -M fragment to the Bi–Bi σ^* orbital. This is the electron pair of b₁ symmetry which is the “extra” (i.e., seventh) pair of the *closo* tetrahedron. This b₁ interaction may be viewed as the cluster counterpart to hypervalency normally associated with single-center heavy main group element compounds such as PF₅. In the PF₅ molecule, a similar orbital results from the donation of an electron pair from F[−] to a σ^* orbital of a PF₄⁺ fragment. There is thus a synergism in the Bi₂– μ -Fe bonding: the metal atom receives an electron pair via the a₁ orbital from the tetrahedron, but it also donates a nonbonding pair in a b₁ orbital to the cluster. The latter donation has no effect on the 18-electron configuration of the metal, since this electron pair remains in the metal coordination sphere. The a₁ electron pair donated to the metal may be better described as a Bi lone pair combination (preserving the Bi–Bi σ bonding), while the b₁ interaction weakens the Bi–Bi bond by partially occupying the Bi–Bi σ^* orbital.

As a result of the three-center nature of the bonding, the Bi– μ -Fe distances (2.896(3) and 2.882(3) Å) are almost 0.2 Å longer than the Bi–Fe distances within the tetrahedral core (2.70 Å, average). The formal addition of the electronically similar Cl⁺ ion (which also requires two additional electrons to fill its valence shell) across the Bi–Bi bond in [4][−] is substantially

(27) Hay, C. M.; Johnson, B. F. G.; Lewis, J.; Raithby, P. R.; Whittan, A. *J. Chem. Soc., Dalton Trans.* **1988**, 2091.

(28) Vites, J. C.; Eigenbrot, C.; Fehlner, T. P. *J. Am. Chem. Soc.* **1984**, *106*, 4633.

(29) Huttner, G.; Schneider, J.; Mohr, G.; von Seyerl, J. *J. Organomet. Chem.* **1980**, *191*, 161.

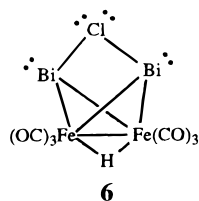
(30) Whitmire, K. H.; Raghuveer, K. S.; Churchill, M. R.; Fettingner, J. C.; See, R. F. *J. Am. Chem. Soc.* **1986**, *108*, 2778.

(31) Curka, P.; Barrett, C. S. *Acta Crystallogr.* **1962**, *15*, 865.

(32) Herschaft, A.; Corbett, J. D. *Inorg. Chem.* **1963**, *2*, 979.

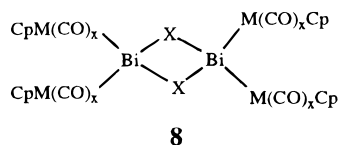
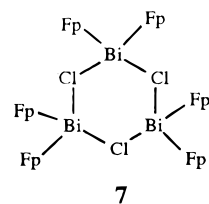
(33) Friedman, R. M.; Corbett, J. D. *Inorg. Chim. Acta* **1973**, *7*, 525.

different owing to its ability also to donate additional lone pairs. This is commonly observed in cluster compounds which incorporate halogen atoms (or halide ions) as bridging ligands. The result would be the hypothetical, neutral $\text{HFe}_2(\text{CO})_6\text{Bi}_2(\mu\text{-Cl})$ (**6**), in which there is no Bi–Bi bond. The actual observed



distance in **[4]**[−] is 3.462(1) Å, well outside the range for Bi–Bi single bonds although still within the van der Waals contact distance of 4.30 Å.³⁴ This hypothetical molecule would be electron precise with 34 electrons as predicted for the metal–metal-bonded dinuclear compound.

The structure of **[4]**[−] is further complicated by the formation of intermolecular hypervalent Bi–Cl interactions so that an extended polymeric network is obtained in the solid state as can be seen in Figure 4. Hypervalency of bismuth atoms which are attached to transition metals as in **[4]**[−] is now well-established in the literature.³⁵ Particularly relevant examples include tetrahedral $[\text{Bi}\{\text{Co}(\text{CO})_4\}_4]^-$,^{9,36} as well as the oligomers $[\text{Fp}^x]_2\text{BiCl}$ (**7**, $\text{Fp}^x = \text{Cp}$ or substituted Cp), which exist in the solid state as cyclic trimers,^{37–39} and $[\text{Cp}(\text{CO})_3\text{Mo}]_2\text{BiI}$ and $[\text{Cp}(\text{CO})_2\text{Mn}]_2\text{BiCl}$, which exist as dimers (**8**)^{40,41} owing to hyper-

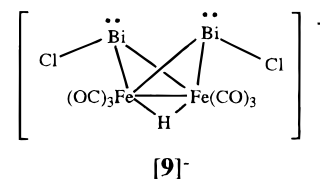


valent Bi–X (X = halide) bonding. Also in this class is the anion $[\text{Fe}(\text{CO})_4\text{Bi}_2\text{Cl}_6]^{2-}$ (**[5]**^{2−}), which will be described in more detail below owing to its relationship to **[3]**^{3−}.²⁶ For **[2]**[−], a weak Bi···Bi intermolecular interaction at 3.610(2) Å is seen. This value is well under the sum of the van der Waals radii and may denote a similar tendency for hypervalency of Bi in **[2]**[−], but this interaction is clearly very weak if even present.

In light of these reports, the Bi–Cl distances deserve some comment. The values associated with the Cl atom intramolecularly bridging the two Bi atoms are 2.876(3) and 2.906(3) Å, and the contacts to the Cl atoms which bridge between cluster units are 2.818(3) and 2.876(3) Å. These values are at the long end of the range found for bismuth chloride complexes^{42–50} and

probably reflect the hypervalent nature of the bismuth atom. It is noteworthy that the intramolecular interactions are, if anything, weaker than those between cluster units. The Bi–Cl interactions for **[4]**[−] must be reasonably strong, however, or $[\text{Et}_4\text{N}][\text{Cl}]$ would be expected to precipitate from solutions using solvents in which that salt is insoluble but in which $[\text{Et}_4\text{N}][\text{4}]$ remains dissolved. The Bi–Cl–Bi angles are quite different for the two types of bridging Cl atoms. For that bridging the Bi–Bi vector, the angle is quite acute (75.56(6) Å), while the intermolecularly bridging Cl ion has a more closely tetrahedral value (101.56(9) Å). Despite these additional perturbations to the tetrahedral core, the Bi–Fe framework remains well-bonded and the resulting Bi–Fe distances (2.654, Å average) are actually significantly (differences $>4\sigma$) shorter than those found in **[2]**[−]. These interactions are similar to the halide ion interactions with the Te atoms in $\text{Te}_2\text{Fe}_2(\text{CO})_6$ recently reported for the solid state structures of $\text{Te}_2\text{Fe}_2(\text{CO})_6 \cdot [\text{Et}_4\text{N}]\text{X}$ (X = Cl, Br).⁵¹ It makes some sense to formulate **[Q][4]** as a double salt of the form **[8]**[−]**[Q][Cl]**, but all attempts made so far to remove the “extra” Cl[−] ligand have failed to give reaction or have led to decomposition.

We believe that the solution structure of **[4]**[−] is different from the solid state structure in that (1) the compound is soluble in common organic solvents and (2) the simple nature of the infrared and NMR spectra is consistent with that expected for a symmetrical anionic compound of the form $[\text{HFe}_2(\text{CO})_6(\mu\text{-BiCl})_2]^-$ (**[9]**[−]). The conversion of **8** to the structure shown



for **[9]**[−] upon addition of Cl[−] in solution is appealing because it allows the molecule to maintain the 34-electron count preferred for dinuclear metal–metal-bonded compounds. The entering Cl[−] ligand is thus accommodated by displacing the lone pair donated by the $\mu\text{-Cl}$ ligand.

An alternative view of **[2]**[−] can be considered by beginning with the *closo*-trigonal bipyramidal $\text{Bi}_2\text{Fe}_3(\text{CO})_9$ molecule, which possesses six skeletal pairs of electrons. Addition of two electrons produces the seven-skeletal-pair system which has the square pyramidal configuration shown as **[10]**^{2−}.⁵² Addition of another ligand produces the bridged-tetrahedral structure **[11]**^{2−} found here in protonated form. This breakage of another Fe–Fe bond upon addition of an electron pair, i.e. on going from **[10]**^{2−} to **[11]**^{2−}, is consistent with bonding expectations, but the transformation is interesting in that the Bi–Bi bonding interaction is retained. This structural conversion was first observed by Rauchfuss for the addition of CO and phosphines

(34) Biondi, A. *J. Chem. Phys.* **1964**, *68*, 441.

(35) Clegg, W.; Compton, N. A.; Errington, R. J.; Fisher, G. A.; Hockless, D. C. R.; Norman, N. C.; Orpen, A. G.; Stratford, S. E. *J. Chem. Soc., Dalton Trans.* **1992**, 3515.

(36) Leigh, J. S.; Whitmire, K. H. *Angew. Chem., Int. Ed. Engl.* **1988**, *27*, 396; *Angew. Chem.* **1988**, *100*, 399.

(37) Wallis, J. M.; Müller, G.; Schmidbaur, H. *J. Organomet. Chem.* **1987**, *325*, 159.

(38) Clegg, W.; Compton, N. A.; Errington, R. J.; Norman, N. C. *J. Chem. Soc., Dalton Trans.* **1988**, 1671.

(39) Clegg, W.; Compton, N. A.; Errington, R. J.; Norman, N. C. *Polyhedron* **1987**, *6*, 2031.

(40) Clegg, W.; Compton, N. A.; Errington, R. J.; Fisher, G. A.; Hockless, D. C. R.; Norman, N. C.; Williams, N. A. L.; Stratford, S. E.; Nichols, S. J.; Jarrett, P. S.; Orpen, A. G. *J. Chem. Soc., Dalton Trans.* **1992**, 193.

(41) von Seyerl, J.; Huttner, G. *J. Organomet. Chem.* **1980**, *193*, 207.

(42) Vezzosi, I. M.; Zanolì, A. F.; Battaglia, L. P.; Corradi, A. B. *J. Chem. Soc., Dalton Trans.* **1988**, 191.

(43) Battaglia, L. P.; Corradi, A. B.; Nardelli, M.; Vidoni Tani, M. E. *J. Chem. Soc., Dalton Trans.* **1978**, 583.

(44) Morss, L. R.; Robinson, W. R. *Acta Crystallogr.* **1972**, *B28*, 653.

(45) Clegg, W.; Errington, R. J.; Fisher, G. A.; Flynn, R. J.; Norman, N. C. *J. Chem. Soc., Dalton Trans.* **1993**, 637.

(46) Mammano, N. J.; Zalkin, A.; Landers, A.; Rheingold, A. L. *Inorg. Chem.* **1977**, *16*, 297.

(47) Aurivillius, B.; Stålhandske, C. *Acta Chem. Scand.* **1978**, *A32*, 715.

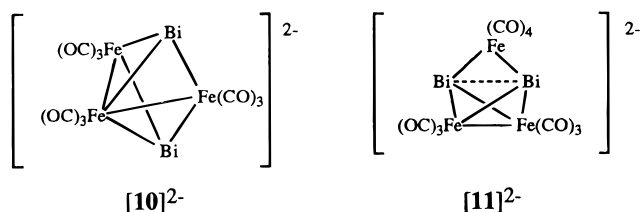
(48) Wiley, G. R.; Collins, H.; Drew, M. G. B. *J. Chem. Soc., Dalton Trans.* **1991**, 961.

(49) Frank, W.; Schneider, J.; Müller-Becker, S. *J. Chem. Soc., Chem. Commun.* **1993**, 799.

(50) Schier, A.; Wallis, J. M.; Müller, G.; Schmidbaur, H. *Angew. Chem.* **1986**, *98*, 742; *Angew. Chem., Int. Ed. Engl.* **1986**, *25*, 757.

(51) (a) Bachman, R. E.; Whitmire, K. H. *J. Organomet. Chem.* **1994**, *479*, 31. (b) Shieh, M.; Shieh, M.-H. *Organometallics* **1994**, *13*, 920.

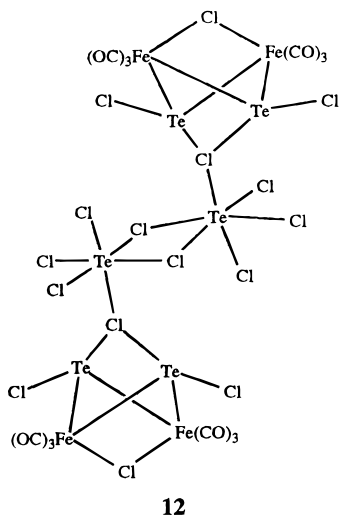
(52) Eveland, J. R.; Whitmire, K. H. *Inorg. Chem.*, in press.



to the square pyramidal Te₂Fe₃(CO)₉, which is isostructural and isoelectronic with [10]²⁻.⁵³ The structure of Te₂Fe₃(CO)₁₀ was recently verified,⁵⁴ and a similar structure has been found for Cp₂Mo₂Fe(CO)₇Te₂.⁵⁵ Because the Te–Te separation in these molecules is approximately the same as the Bi–Bi distance in [2]⁻, the degree of interaction for the chalcogenide system is correspondingly weaker since Te is a smaller atom.

One other view for these bridged-tetrahedral clusters should be considered. This structure is based upon an *arachno*-pentagonal bipyramidal parent, as predicted by the presence of eight skeletal electron pairs. The view has some merit but again does not account for the substantial Bi–Bi bonding observed. This issue has been previously analyzed by extended Hückel calculations and discussed in some detail.²⁴

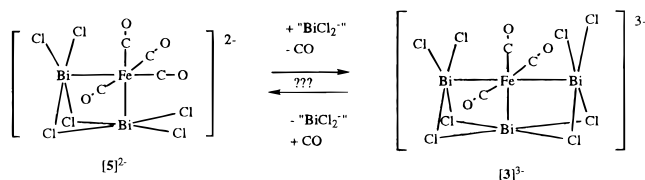
We note also that the coordination geometry around the bismuth center in [4]⁻ is similar to that recently reported for the related Fe–Te compound [Fe₂(CO)₆(μ-Cl)(μ-TeCl₂)₂Te₂-Cl₁₀] (12).⁵⁶ In 12, a Fe₂Te₂ core with a butterfly geometry is



observed with one terminal chloride ligand on each Te atom and one chloride ligand bridging the two tellurium centers, very similar to the coordination geometry observed for the bismuth centers in [4]⁻. The Cl_{terminal}–Te–Cl_{bridge} angle in 12 (173.36(7)°, average) is close to the corresponding angles in [4]⁻ (165.85°, average).

The structure of [3]³⁻ is unique (Figure 2). At first glance, it may be viewed as a simple Fe(CO)₃ fragment coordinated to a complex [Bi₃Cl₈]³⁻ moiety, although the distribution of charge between the Fe and Bi fragments is not straightforward, as will be discussed momentarily. The coordination environment about iron is that of a conventional octahedron, and that for the bismuth atoms is a square pyramid with a lone pair of electrons expected to occupy the sites *trans* to the Bi–Fe bonds. The

Scheme 2



angles around each bismuth atom are reasonably regular and close to the anticipated value of 90° for the square pyramidal arrangement. The greatest distortion occurs around Bi(2). This geometry about bismuth is commonly seen in a variety of hypervalent bismuth(III) coordination compounds. The Bi–Cl bond distances are, however, very asymmetrical, falling into three general groups: Bi(1,3)–Cl_{terminal} (2.616 Å, average) < Bi(2)–Cl_{bridge} (2.798 Å, average) < Bi(1,3)–Cl_{bridge} (3.084 Å, average). Given the long Bi(1,3)–Cl_{bridge} distances, the fragment may perhaps be viewed more appropriately as being composed of two BiCl₂ units and one BiCl₄ group. The Bi(1,3)–Cl_{terminal} distances are within the range normally found for such complex ions,^{42–44,57} while the distances to the bridging Cl atoms are significantly longer but still consistent with values associated with hypervalent bismuth compounds having bridging halides. As with most hypervalent complexes, there is a give-and-take in the bond distances such that the average of the long and short bonds to Bi(1) and Bi(3) is 2.850 Å, which is not significantly different, according to the error bars on these data, from the average for the four Bi(2)–Cl_{bridge} bonds.

There is an obvious relationship between the structure of [3]³⁻ and that of [Fe(CO)₄Bi₂Cl₆]²⁻ ([5]²⁻) reported earlier (Scheme 2).²⁶ Replacing a CO ligand on [5]²⁻ with a BiCl₂⁻ fragment will achieve the production of [3]³⁻. Bismuth has a formal oxidation state of +1 in BiCl₂⁻; while this oxidation state has been found for reduced bismuth halides in the solid state compounds, it is not documented for discrete bismuth halide compounds except in transition metal systems like [{CpMn(CO)₂]₂BiCl₂},⁴¹ where the oxidation state assignments are ambiguous. It is not unreasonable, however, that BiCl₂⁻ might have a fleeting existence, which would allow for a direct substitution as shown in Scheme 2, especially given that both complexes have been isolated from this same reaction system. Preliminary attempts, however, to convert [5]²⁻ into [3]³⁻ or vice versa have not been successful. Since (1) the reaction is complicated, giving a mixture of products, (2) [3]³⁻ has a limited solution stability, and (3) there are no convenient spectroscopic handles to probe the system, we have not yet been able to devise experiments that would answer this mechanistic question.

A simple consideration of electron counting in [Bi₃Cl₈]³⁻ shows immediately that the bismuth atoms must be in a reduced oxidation state. The simple back-of-the-envelope calculation gives an average oxidation state of 5/3⁺ for each bismuth atom. In order to explore this unusual condition more thoroughly, EH calculations were performed on [3]³⁻, which were more consistent with the a 7/3⁺ oxidation state, as detailed below.

Theoretical Study of [3]³⁻. We first consider an idealized C_{2v} structure for the anion [3]³⁻, in which all bond angles around the Fe and Bi atoms are equal to 90 or 180°. Thus, in this geometry, Bi(1) is perfectly square planar, while Fe is perfectly octahedral. Figure 5 shows the MO diagram of [3]³⁻, based on the interaction between the Fe(CO)₃ and Bi₃Cl₈ fragments. The frontier orbital set of a T-shaped unit such as the Fe(CO)₃

(53) Lesch, D. A.; Rauchfuss, T. B. *Organometallics* **1982**, *1*, 499.

(54) Gervasio, G. J. *Organomet. Chem.* **1992**, *441*, 271.

(55) Bogan, J. L. E.; Rauchfuss, T. B.; Rheingold, A. L. *J. Am. Chem. Soc.* **1985**, *107*, 3843.

(56) Eveland, J. R.; Whitmire, K. H. *Angew. Chem.* **1996**, *108*, 841; *Angew. Chem., Int. Ed. Engl.* **1996**, *35*, 741.

(57) Drew, M. G. B.; Nicholson, D. G.; Sylte, I.; Vasudevan, A. *Inorg. Chim. Acta* **1990**, *171*, 11.

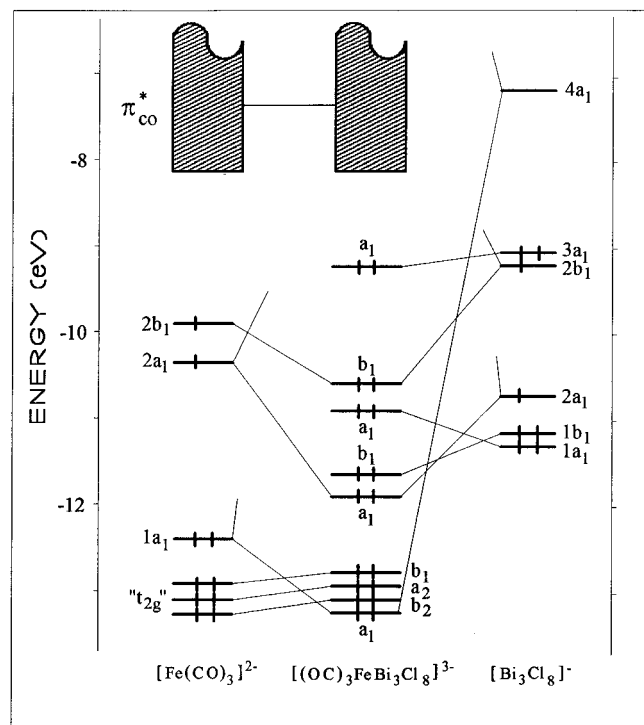


Figure 5. MO diagram of the $[\text{Fe}(\text{CO})_3\text{Bi}_3\text{Cl}_8]^{3-}$ C_{2v} model, based on the interaction of the $[\text{Fe}(\text{CO})_3]^{2-}$ (left) and $[\text{Bi}_3\text{Cl}_8]^-$ (right) fragments.

fragment is well-known.^{58,59} It is composed of the six levels drawn on the left side of Figure 5. Three of them ($1a_1$, $2a_1$, and $2b_1$) are plotted at the bottom of Figure 6. The two highest are hybrids of y/yz and $s/z/z^2$ character. The former, $1b_1$, points toward Bi(2) and Bi(3), while the latter, $2a_1$, points toward Bi(1). Below these two hybrids lies a group of d-type levels, of which the highest, $1a_1$, is of y^2 character. Among these six levels of the $\text{Fe}(\text{CO})_3$ fragment, only the three highest ($1a_1$, $2a_1$, and $2b_1$) have the proper directional properties to interact with the Bi atoms. The lower three will not interact with the Bi atoms, giving rise to the nonbonding "t_{2g}" set of the octahedrally coordinated Fe atom in $[\text{Fe}(\text{CO})_3\text{Bi}_3\text{Cl}_8]^{3-}$.

Similarly, the Bi_3Cl_8 fragment has six frontier orbitals (right side of Figure 5), of which three will be mainly involved in the interaction with the Fe atom. These six levels (plotted at the top of Figure 6) can be constructed from the combination of the frontier orbitals of two bent BiCl_2 units and one square planar BiCl_4 unit. Each BiCl_2 fragment possesses two frontier orbitals,⁵⁹ one of pure p type pointing toward the Fe atom and one sp hybrid pointing "down", in the BiCl_2 plane. The square planar BiCl_4 unit has two frontier orbitals⁵⁹ located on Bi(1) with some chlorine antibonding admixture respectively of z and s dominant character. When the three Bi fragments are put together, one obtains the energy level ordering shown in the right side of Figure 5. The s-type orbital on Bi(1) remains almost unperturbed, generating the $3a_1$ level of the Bi_3Cl_8 fragment. The sp hybrids of Bi(2) and Bi(3) mix to form an in-phase ($1a_1$) and an out-of-phase ($1b_1$) combination. A similar situation occurs with pure p-type orbitals on Bi(2) and Bi(3), giving rise to the $2a_1$ and $2b_1$ levels. However, the in-phase $2a_1$ combination overlaps somewhat with the z-type level of Bi(1), acquiring some bonding admixture of this level, while the latter ($4a_1$) acquires some antibonding admixture of the former. This mixing may be overestimated by the calculations

because of an overestimation of the overlap between the nonbonded Bi atoms. When the $\text{Fe}(\text{CO})_3$ and Bi_3Cl_8 fragments interact, the $1a_1$, $1b_1$, and $3a_1$ levels of Bi_3Cl_8 , which point *trans* to the Fe atom, remain mainly nonbonding, housing the three Bi lone pairs. The $4a_1$ and $2a_1$ levels of Bi_3Cl_8 interact with the $1a_1$ and $2a_1$ metallic level (mainly $4a_1$ with $1a_1$ and $2a_1$ with $2a_1$). Another strong bonding interaction occurs between $2b_1$ of Bi_3Cl_8 and $2b_1$ of $\text{Fe}(\text{CO})_3$. Clearly, the bismuth-iron interactions can be described within a localized two-electron/two-center scheme. After interaction, the populations in the $1a_1$ and $2a_1$ levels of $\text{Fe}(\text{CO})_3$ are 1.50 and 1.01, respectively, with corresponding values of 1.21 and 0.57 in the $2a_1$ and $4a_1$ orbitals on the Bi_3Cl_8 fragment. Then, one a_1 bonding pair can be formally considered as originating from the y^2 metallic orbital, while the other one is fairly equally distributed on the two fragments. The populations of the b_1 orbitals are 0.94 and 1.10 for the metal and bismuth fragments, respectively. Again this is a rather nonpolar interaction. From these results we propose the formal occupation of the frontier orbitals before interaction shown in Figure 5. It corresponds to an oxidation state of 2- for Fe and $7/3+$ for the Bi atoms. There is no clear need to attribute two different oxidation states to the two types of Bi atoms. Their calculated net charges are close, respectively 1.16 and 1.13 for Bi(1) and Bi(2,3). The net charge of Fe (-1.24) is also in agreement with the proposed oxidation state, keeping in mind that the formal -2 charge before interaction is significantly reduced by the strong Fe-Bi covalent interactions, as well as the Fe-CO interactions (in the isolated $[\text{Fe}(\text{CO})_3]^{2-}$ anion, the computed Fe net charge is -1.65). These findings are in agreement with our initial postulate and calculations for the related $[\text{Fe}(\text{CO})_4\text{Bi}_2\text{Cl}_6]^{2-}$ molecule,²⁶ wherein the iron carbonyl fragment functions as a pseudohalide, donating electrons to the hypervalent bismuth atoms.

We now turn the discussion to the analysis of the long Bi-(2,3)···Cl bonding contacts. In the considered C_{2v} model, the Bi(2,3)···Cl distances (3.34 Å) are longer than the experimental ones. Consistently, the corresponding overlap populations are very small, but positive (+0.008), indicating a weak bonding interaction. In the experimental structure, the Bi(2,3) atoms bend slightly toward the Bi(1)Cl₄ unit and the ClBi(1)Cl angles are distorted from 90°, in such a way that the Bi(2,3)···Cl distances are shorter. When we apply this distortion to our model while maintaining the C_{2v} symmetry, the Bi(1,2)···Cl distances are shortened (3.11 Å) and the corresponding overlap populations are larger (+0.016), due to a better overlap between the $\sigma^*(\text{BiCl}_2)$ orbitals and the Cl p lone pairs of the square planar BiCl_4 unit. Clearly, these results are consistent with a tendency to hypervalency for Bi(2) and Bi(3). However, it is likely that the bonding energy associated with the Bi(1,2)···Cl contacts is somewhat underestimated in the EHMO calculations. Calculations carried out on the experimental structure of $[\text{Fe}(\text{CO})_3\text{Bi}_3\text{Cl}_8]^{3-}$ lead to results that are very similar to those obtained with the "distorted" C_{2v} geometry. The main difference concerns the energy of the Bi(1) lone pair (HOMO of $[\text{Bi}_3]^{3-}$) which is, because of a better s/z hybridization, close to the energies of the other Bi lone pairs in the experimental structure, rendering these three lone pairs chemically equivalent.

Phosphorus-Containing Byproducts. As is clear from the isolation of the title compounds from the reaction of $[\text{I}]^{2-}$ with MePCl_2 , no phosphorus has been incorporated into the resulting metal-containing products. During the isolation of the clusters, it was noted that the washes of the compounds contained foul-smelling residues reminiscent of phosphine complexes, and so an effort was made to isolate those compounds and determine their nature. During the workup, it was clear that these materials

(58) Hoffmann, R. *Angew. Chem., Int. Ed. Engl.* **1982**, *21*, 711.

(59) Albright, T. A.; Burdett, J. K.; Whangbo, M.-H. *Orbital Interactions in Chemistry*; John Wiley and Sons: New York, 1985.

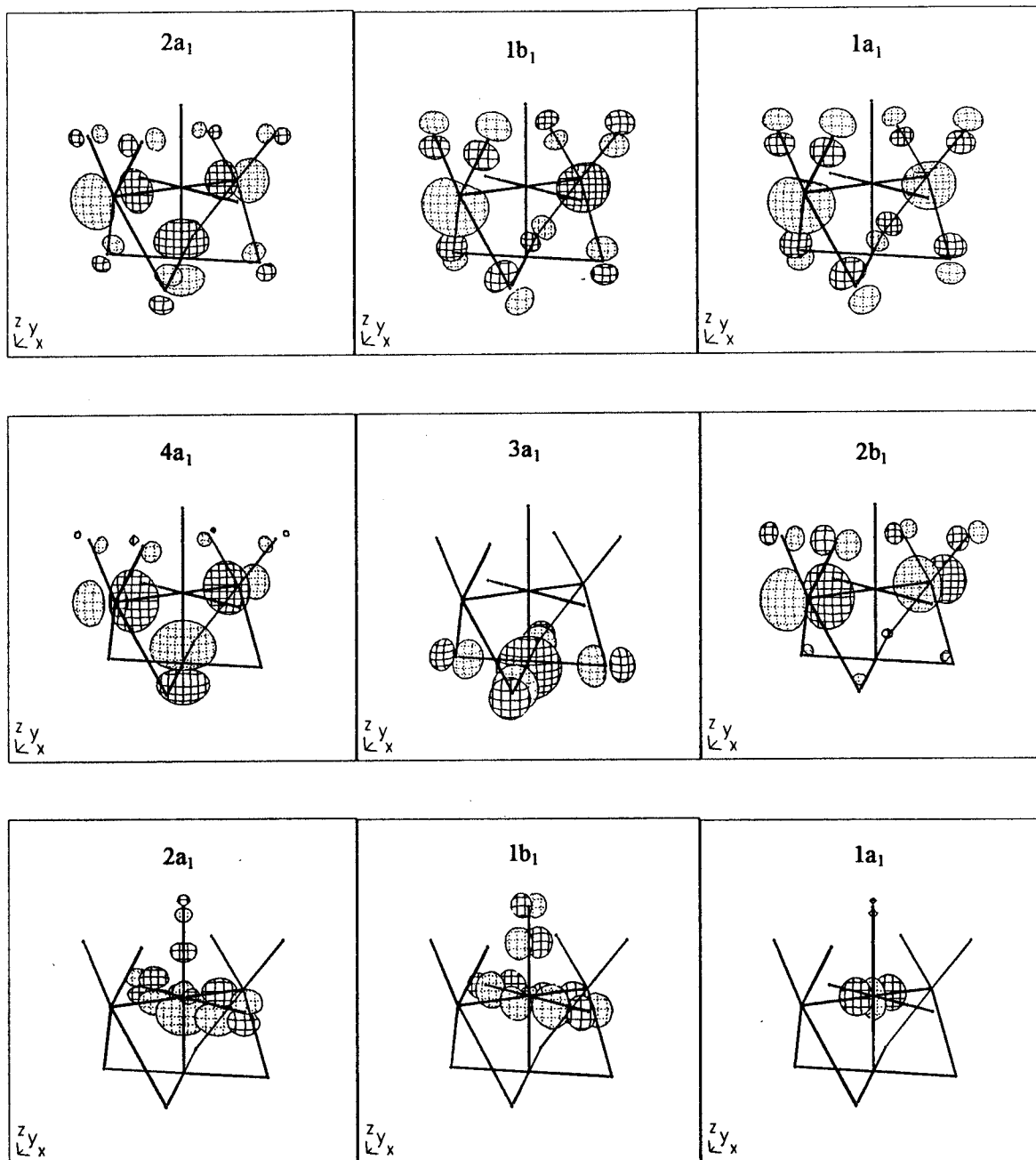
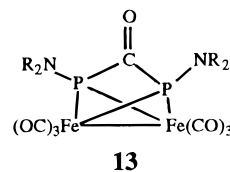


Figure 6. CCAO4.0 plots of the major fragment frontier orbitals of the Bi_3Cl_8 (top) and $\text{Fe}(\text{CO})_3$ (bottom) fragments.

could be separated into more and less volatile fractions of colorless liquids, with the latter being somewhat viscous and considerably higher boiling. The mass spectral data showed that the highest masses for both were in a similar range (m/e 1117, 1113) consistent with the formation of polymeric materials. The mass spectra showed a regular loss of 74–75 mass units for both fractions, which could correspond to a variety of fragments that could arise in this reaction, including Me_3P , $-\text{P}-\text{CH}_2-\text{P}-$, $-\text{P}(\text{H})-\text{CH}_2-\text{C}(\text{=O})-$, or $-\text{C}(\text{=O})-\text{P}(\text{H})-\text{CH}_2-$. The more volatile fraction 1 gave an NMR spectrum which indicated the presence of P–H bonds ($J_{\text{P-H}} = 533$ Hz), but such functional groups were missing in fraction 2. The NMR data did not indicate the incorporation of solvent THF, however. Metal carbonyl groups appear to be lacking in both fractions, as determined by the infrared spectra, but the fractions do contain bands in the organic carbonyl region (1653 cm^{-1} for fraction 1 and 1643 cm^{-1} for fraction 2), which suggested the presence of fragments such as $-\text{C}(\text{=O})-\text{P}(\text{H})-\text{CH}_2-$, $-\text{P}(\text{H})-\text{CH}_2-\text{C}(\text{=O})-$, or $-\text{P}(\text{R})-\text{C}(\text{=O})-\text{P}(\text{R})-$. The peak positions

of these absorptions correlate well with those reported by King *et al.* for some iron–phosphine species with bridging $-\text{P}-\text{C}(\text{=O})-\text{P}-$ groups (**13**).⁶⁰ A series of compounds of general



formulas $\text{Fe}_2(\text{CO})_6\{\text{R}_2\text{NP}\}_2\text{CO}$ and $\text{Fe}_2(\text{CO})_6\{\text{R}_2\text{NP}\}_3\text{CO}$ were prepared via the similar reaction of R_2NPCL_2 with $[\text{Fe}(\text{CO})_4]^{2-}$. These results suggest that metalation and carbonylation of the methylchlorophosphine may in fact occur in our system in spite of our inability to isolate metal complexes which retain phosphorus. If such complexes are unstable, it is reasonable

(60) King, R. B.; Wu, F.-J.; Holt, E. M. *J. Am. Chem. Soc.* **1987**, *109*, 7764.

to assume that they could decompose with formation of polymeric phosphine complexes.

As far as we know, the nature of the non-metal carbonyl phosphine byproducts in reactions of $[\text{Fe}(\text{CO})_4]^{2-}$ (or other metal carbonylate anions) has not been investigated, and this promises to be an interesting research problem in its own right. Given the low yields of these materials, their complex nature, and the synthetic difficulties in preparing them from $[\mathbf{1}]^{2-}$, we have chosen not to pursue more detailed characterization of fractions 1 and 2 obtained by this methodology but are exploring the possibility that reactions with more easily obtained metal carbonylate dianions such as $[\text{Fe}(\text{CO})_4]^{2-}$, $[\text{Fe}_2(\text{CO})_8]^{2-}$, and $[\text{Fe}_3(\text{CO})_{11}]^{2-}$ will lead to similar polymeric species.

Acknowledgment. The National Science Foundation (K.H.W.), the Robert A. Welch Foundation (K.H.W.), and the Centre National de la Recherche Scientifique (J.-Y.S.) are gratefully acknowledged for financial support of this work. The NSF and CNRS are also thanked for a joint travel grant to facilitate this collaboration.

Supporting Information Available: X-ray crystallographic files, in CIF format, for $[\text{Et}_4\text{N}][\mathbf{2}]$, $[\text{PhCH}_2\text{NMe}_3]_3[\mathbf{3}] \cdot 0.87\text{Et}_2\text{O}$, and $[\{\text{PhCH}_2\text{NMe}_3\}_4]_\infty$ are available on the Internet only. Access information is given on any current masthead page.

IC9609721